Available online at www.sciencedirect.com
ScienceDirect
Ceramics International 34 (2008) 107–112
CERAMICS INTERNATIONAL
www.elsevier.com/locate/ceramint

Porous ceramics with tri-modal pores prepared by foaming and starch consolidation

Xiaojian Mao [a,b], Shiwei Wang [a,*], Shunzo Shimai [a]

[a] *Shanghai Institute of Ceramics, Chinese Academy of Sciences, Shanghai 200050, PR China*
[b] *Graduate School of Chinese Academy of Science, Beijing 100039, PR China*

Received 15 June 2006; received in revised form 7 July 2006; accepted 21 August 2006
Available online 2 October 2006

Abstract

Porous silica ceramics with tri-modal pores were prepared, based on the generation of foams from silica/starch composite slurry and the subsequent stabilization of the structure by starch consolidation. The rheology of the original slurry and the foamed one were evaluated and compared. After drying, the green bodies were debindered and sintered at 1250 °C for 5 h. The resulting materials consisted of a hierarchical structure with large-sized cells, moderate-sized pores in cell wall and small-sized voids among silica grains. The compressive strength of the sintered samples varied within the range of 4–17 MPa, corresponding to relative densities of 18–30%.

Keywords: C. Strength; D. SiO_2; Porous ceramics; Foaming; Microstructure

1. Introduction

There is currently widespread interest in porous ceramics for their specific properties, such as low bulk density, low specific heat, low thermal conductivity, high surface area and high permeability [1–3]. These properties are expected of technological applications which include filters for molten metals, catalyst carriers, thermal insulation, lightweight structural materials, biomaterials and so on [4–7]. In addition to the composition of porous ceramics, the morphology, porosity and pore size distribution, which are determined by preparation processing, are also important factors that dominate the suitability for potential applications [8,9]. Predominantly closed pore ceramics are needed for thermal insulation while open pore ceramics are required for fluid transport, such as metal filters [9]. Micropores are suitable for sewage purification [10], while macropores are necessary for bone implantation [11]. A combination of different morphologic pores in a designed monolithic matrix could be expected to extend the properties of porous ceramics and subsequently outspread the application fields [12].

So far, a number of routes, such as polymeric sponge replication, direct foaming, adding fugitive granules, sintering of hollow spheres and sol–gel systems have been developed for the preparation of porous ceramics [3,13]. However, these routes are usually available for pores with certain morphology and scale. For example, polymeric sponge replication is the most common approach for producing reticulated porous ceramics with pore sizes varying from approximately 100 μm to 5 mm [2]. Chemical techniques, such as sol–gel systems, make the fabrication of nano-pores attainable and facile [14,15].

This work describes studies on a novel processing route for porous ceramics with hierarchical structure of tri-modal pores. The technique comprises the foaming of aqueous ceramic slurries containing starch prior to the consolidation of the foam.

2. Experiment

2.1. Materials

Silica powder used in the present study, with a mean particle size of 3.8 μm, was prepared by ball-milling silica glass. Lactic acid was adopted as dispersant. A commercial liquid detergent WhiteCat® (cationic surfactant, Shanghai WhiteCat Co., Ltd., China) was used as foaming agent. Sodium carboxymethylcellulose (CMC) was employed to modify the rheological

* Corresponding author. Tel.: +86 21 52414320; fax: +86 21 52413903.
E-mail address: swwang51@mail.sic.ac.cn (S. Wang).

0272-8842/$32.00
doi:10.1016/j.ceramint.2006.08.009

property of the slurry, as well as to stabilize foams. The cassava starch (DF, Shanghai DF Candy Co., Ltd., China), with a mean particle size of 18 μm and a density of 1.43 g cm^{-3}, was used to consolidate the foams.

2.2. Preparation processing

The schematic diagram of processing is described in Fig. 1. Silica powders, 0.2 wt% CMC and 10 wt% cassava starch based on silica powders were added to distilled water to prepare slurry by a planetary ball milling for 30 min. Lactic acid was added to adjust the pH value of slurry to 3–4 [16]. The total solid loading was varied from 62.9 to 71.0 wt%, to gain samples with different relative densities. After adding the forming agent WhiteCat®, these slurries were vigorously whisked with an electric beater at a stirring rate of 750 rpm in a plastic beaker for about 5 min. After foaming, the as-foamed slurries were immediately poured into polypropylene molds (110 mm × 65 mm × 30 mm), which were then covered with plastic film to reduce water evaporation.

The filled molds were preheated in a microwave oven with a power of 400 W for 60 s, and then moved into a 70 °C-oven for 30 min. After consolidation and a slow cooling, the wet bodies were demoulded and left at room temperature for 36 h, and then stored at 50–80 °C for 2–3 days. The complete drying was performed at 120 °C.

Burn-out was accomplished by heating in air at a rate of 1.0 °C min^{-1} up to 500 °C, assisted by holding at 300 °C for 2 h to avoid violent pyrogenation. Finally, the sintering was performed in air at 1250 °C for 5 h.

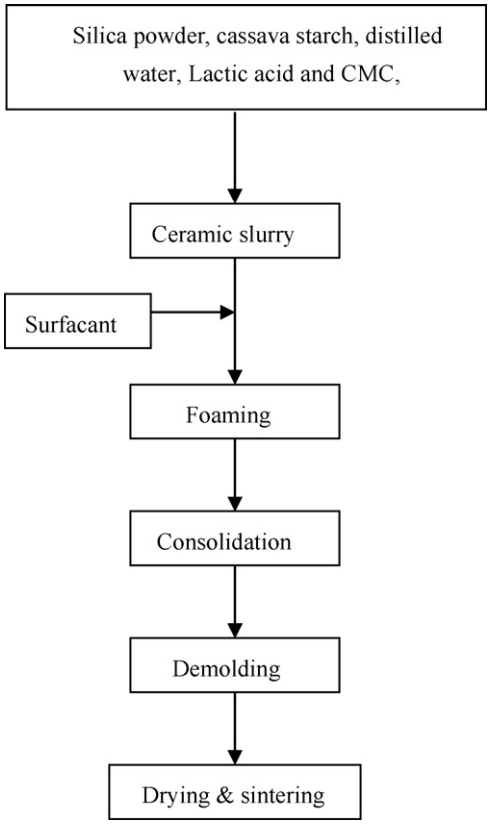

Fig. 1. Flow-chart of process for porous silica ceramics using foaming and starch consolidation method.

2.3. Characterization

The rheological property of the original and foamed slurries were measured by a stress-controlled rheometer (Model SR50, Rheological Scientific Inc., USA) with a parallel plate (25 mm in diameter), using the steady-shear measurement at 25 °C. Differential scanning calorimetry and thermogravimetry (DSC/TG, Netzsch Sta 449C) were carried out to understand the details of the starch burn-out at the rate of 10 °C min^{-1}. Relative density of sintered ceramics was determined through the ratio of mass and dimension of sintered samples. Compressive strength was measured using an Instron-1195 universal testing machine with a cross head speed of 1 mm min^{-1}. The dimension of the test piece was 15 mm × 15 mm × 15 mm. The cross-sectional area of the sample and the maximum failure load were used to calculate the fracture stress. The microstructure of the samples was observed by scanning electron microscopy (SEM, JSM-5600LV, Japan). Size distribution of large-sized cells within the sintered samples was obtained by statistical analysis of SEM micrographs. The observed areas were approximately 3 mm^2.

3. Results and discussion

3.1. Foaming of slurry

The evolution of the foaming capacity versus the concentration of the surfactant is shown in Fig. 2. The solid loading of the original slurry was 62.9 wt%. The foaming capacity strongly increases until it reaches a maximal value, and then undergoes a plateau with a slight decrease. During the initial stirring period air, is entrained into the slurry and fresh surface is formed. Subsequently, the surfactant molecules of the

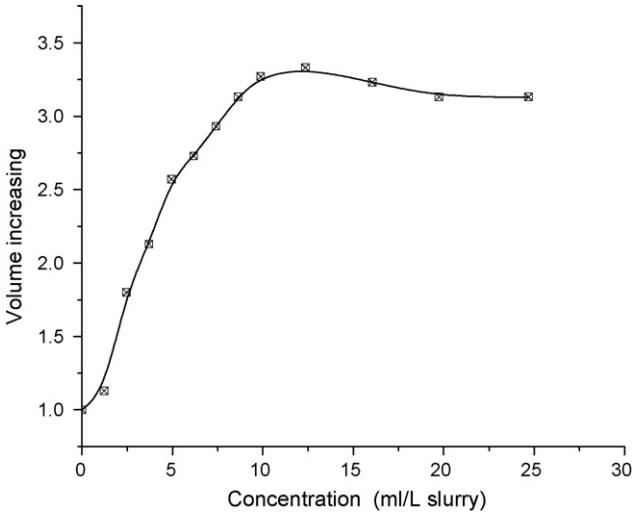

Fig. 2. Evolution of the foaming capacity vs. the concentration of the surfactant based on slurry. The solid loading of the original slurry was 62.9 wt%.

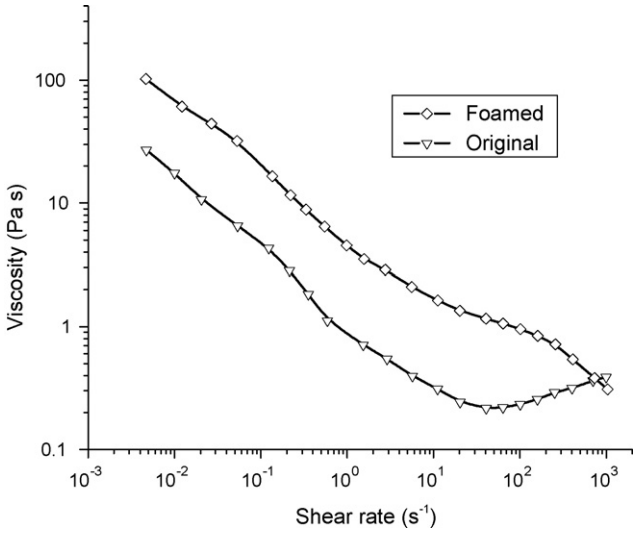

Fig. 3. Rheological behaviors of slurry before and after foamed with a solid loading of 45 vol%.

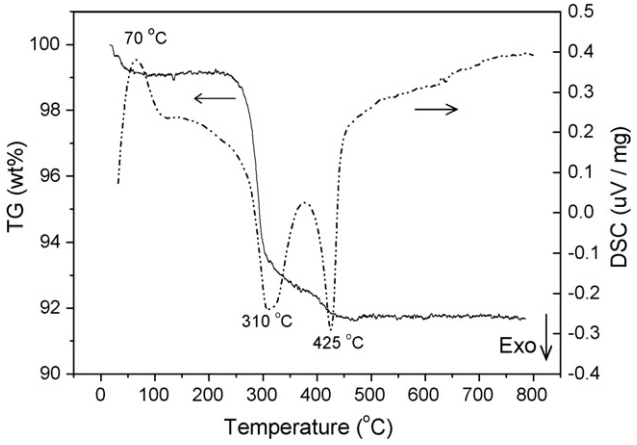

Fig. 4. TG/DSC curves for thermal behavior of dried body in air.

foaming agent transfer from interior of the slurry towards the newly created surface, decreasing the surface tension which will favor foaming. Increasing the surfactant concentration accelerates this transfer, and hence increases the foaming capacity. For a certain concentration, the transfer effect equivalent with the creasing rate of the new surface and the foaming capacity is maximal. For a higher concentration, the surface tension remains minimal, but the presence of more surfactant will increase the viscosity of slurry, which will inhibit the foaming effect. From Fig. 2, the optimal surfactant addition of 1.2 vol% based on slurry was employed for all other foaming process.

Fig. 3 presents plots of viscosity as a function of shear rate for the original slurry and the foamed one with a total solid loading of 68.8 wt%. For the original slurry, a clear shear-thin behavior appeared and then a slight shear-thick behavior followed, as typical behavior of concentrated suspensions [17]. The foamed slurry was of much higher viscosity than the original one, at the low shear rate measured. It can be attributed to the presence of bubbles and surfactant molecules at the gas–liquid interfaces. The transformation of spherical bubbles into elliptical at the low shear flow resulted in the increasing of these interfaces, which provided resistance to deformation, corresponding to higher viscosity. However, at the higher shear rate the foamed viscosity kept decreasing as well and attained values that were less than that of original slurry. The bubbles thoroughly collapsed and became slip gas layers at high shear rate, resulting in low apparent viscosity. The crossing point of viscosity was related to the stress level of original foaming whisk. A higher viscosity of foams at low shear rates was advantageous to the stabilization of bubbles. However, if the viscosity was over high, it was not convenient for casting because of the relatively low density of foams.

3.2. Burn-out

In general, foamed green body is easy to debinder than dense body, for it contains abundant cells and channels to let pyrolysates occupy and escape. Thermal analysis was used to optimize the burn-out schedule of the foamed body. Fig. 4 shows the TG and DSC curves for a dried body carried out in air. Firstly, absorbed gas and water was removed from room temperature to about 120 °C, with 1 wt% weight loss and an endothermic peak at 70 °C. The starch would undergo weight reduction at two stages: a remarkable loss of about 6 wt% occurred at about 310 °C, and a following slight decrease continued to about 480 °C. This result is confirmed by the DSC curve, with two exothermic peaks at 310 and 425 °C, respectively. At these two stages, heating rate should be slow enough to avoid over violent pyrogenation. Based on this result, the optimized thermal schedule for the firing of the bodies could be determined in Section 2.2.

3.3. Density and microstructure

Sintered ceramics prepared in this work exhibited relative densities in the range of 18–30%, increased with varying solid loadings of 62.9–71.0 wt%, as shown in Fig. 5. It can be explained that high solid loading of the slurry resulted in high

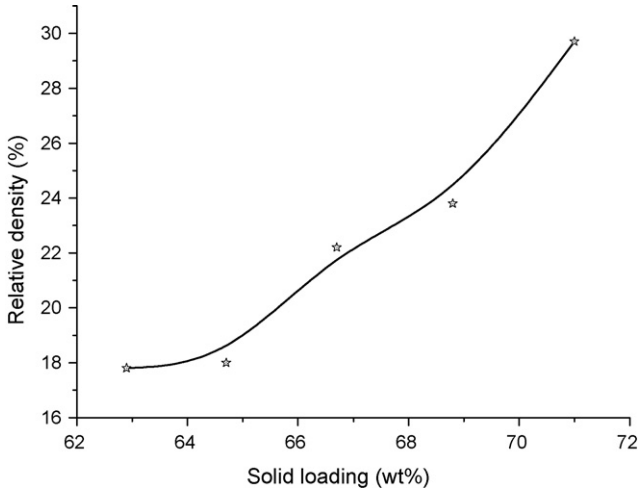

Fig. 5. Relative density of sintered ceramics varies with solid loading of original slurries.

viscosity, hence decreased the foaming capacity. Besides, high solid fraction itself also led to high density of cell struts.

Fig. 6 shows the microstructure feature of sintered ceramics. A tri-modal hierarchical structure is composed by large-sized cells larger than 50 μm, moderate-sized pores in walls averaging about 10 μm (Fig. 6(a)) and small-sized voids (Fig. 6(b)). It can be inferred that the large-sized cells, moderate-sized pores and small-sized voids were originated from bubbles, elimination of starch particles and interstices among the silica grains, respectively. The large-sized cells were mainly attributed to the bubbles in foams. The moderate-sized pores acted as channels between cells and their size can be easily controlled by starch particles. These channels are essentially required in the use for catalyst supports and biomaterials because they sieve mass transfer between contiguous cells. The small-sized voids will increase the specific surface area of ceramic matrix.

Generally, relative density remarkably affected the cell morphology of porous ceramics fabricated by foaming method [18,19]. Highly foamed slurries lead to the final foams containing larger cells and more cell windows, while a structure with smaller window size even absolutely closed cells was derived as the density increased [8,20]. In this case, however, the cell morphologies are almost the same, for relative densities varying from 18 to 30%, except for a little variation of the cell sizes, as illustrated in Figs. 7 and 8. The sintered ceramics showed approximately spherical cells with no preferred orientation. The requirement of ceramic foams with similar morphologies but different porosities could be satisfied by this method.

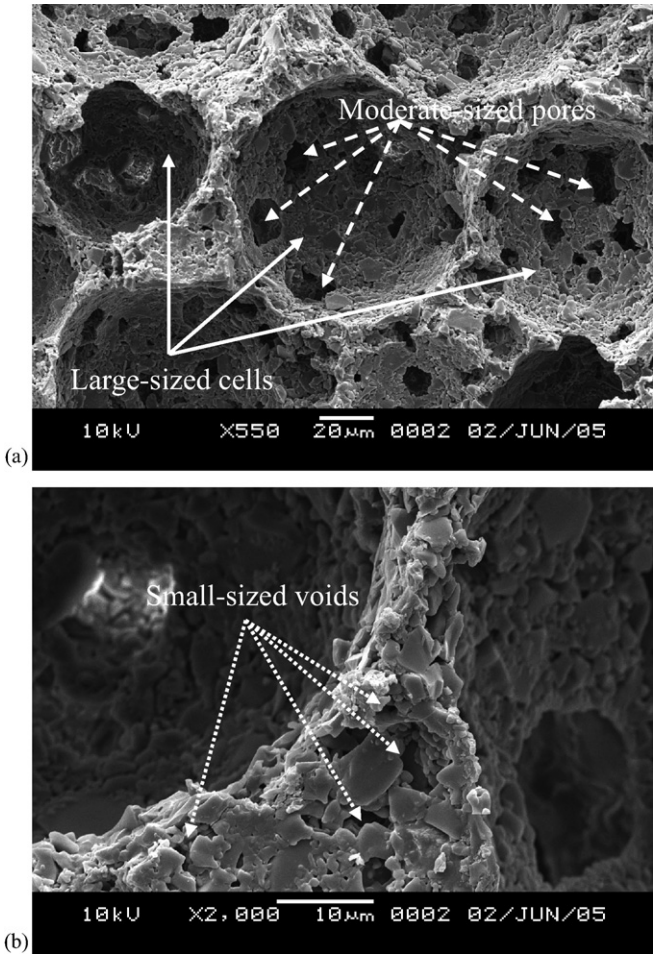

Fig. 6. SEM micrographs of sintered sample consist of: (a) large-sized cells and moderate-sized pores, and (b) small-sized voids.

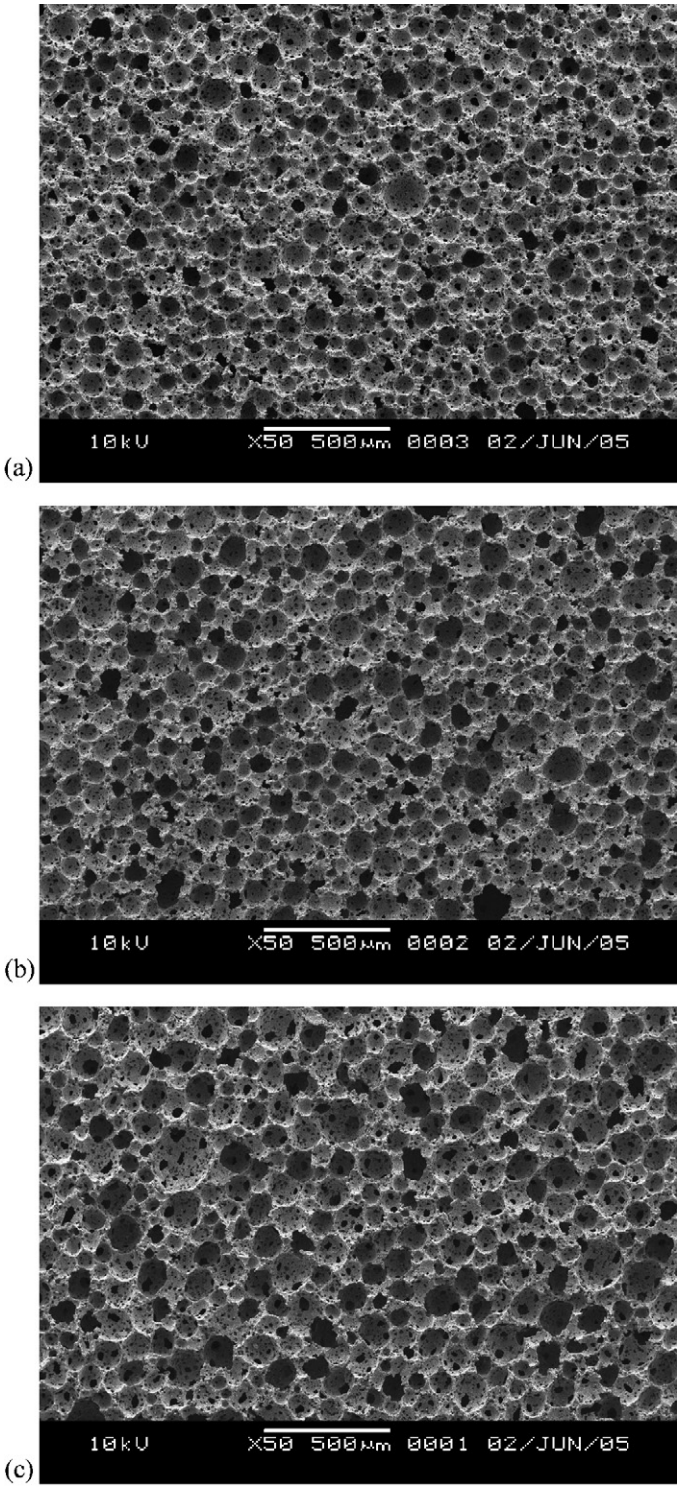

Fig. 7. SEM micrographs of sintered samples with a relative density of: (a) 30%, (b) 22% and (c) 18% of theoretical.

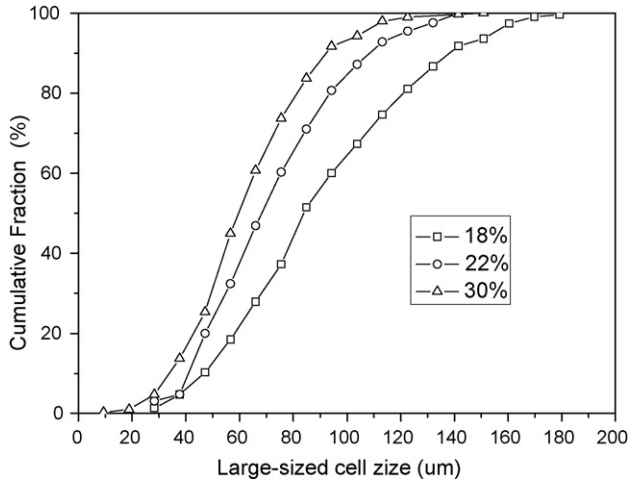

Fig. 8. Cell size distributions of large-sized cells at various relative densities.

3.4. Mechanical strength

The compressive strength of porous silica ceramics varied within the range of 4–17 MPa, as shown in Fig. 9. As expected, the strength decreases proportionally to the decrease in density owing to the larger volume fraction in lower density specimens [21]. Ashby's theory indicates that the strength of a cellular material (σ) is related to its relative density (ρ/ρ_s) via the expression

$$\frac{\sigma}{\sigma_s} = K\left(\frac{\rho}{\rho_s}\right)^m \quad (1)$$

where σ_s is the strength of the strut material, K dimensionless constant and the exponent m is 3/2 or 2, depending on if the cell morphology is open cell or closed cell, respectively. In our case, the morphology of the ceramics, as shown in Fig. 7, is much more similar with closed foams, containing connected pores in the cell wall. Thus, it is reasonable that the strength data for our samples are more descriptive to what the model predicts for closed-cell foams. The relationship between relative density and compressive strength in present case had a slope of $m = 2.4$ in a double log plot. It is much smaller than the value obtained by Colombo et al. [20] and Oliveira et al. [21], although a little bigger than 2 the value predicted by Ashby's model. The closer to Ashby's theoretical value results from more uniform microstructure. And the remaining lack of rigorous fit may be mainly due to the inhomogeneous cell sizes (a cell size distribution) and the still change of average cell size with relative density, as shown in Fig. 8.

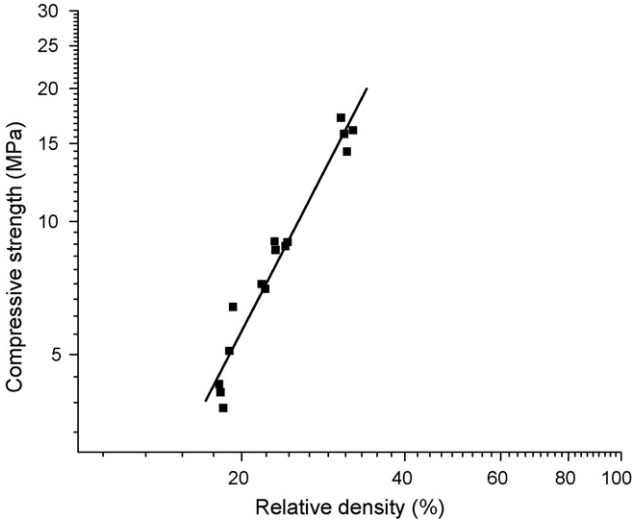

Fig. 9. Double log plot of relationship between relative density and compressive strength.

4. Conclusions

A novel method was developed to make porous ceramics with hierarchical structure by foaming and starch consolidation. The viscosity of the foamed slurry was higher than that of the original slurry at a low shear rate, but lower at a high shear rate. The density of the ceramic could be varied by altering the solid loading of the slurry. Porous silica ceramics with relative density of 18–30% and compressive strength of 4–17 MPa were obtained from slurries with solid loading of 62.9–71.0 wt%. The resulting ceramics consisted of tri-modal pores of large-sized cells, moderate-sized pores in cell wall and small-sized voids among silica grains. This new kind of processing method will extend the potential application of porous ceramics.

Acknowledgement

The authors would like to thank Mr. M.J. Dong (State Key Lab of Supermicrostructure and High Performance Ceramics of SICCAS) for his help in the evaluation of rheology.

References

[1] F. Carn, A. Colin, M.F. Achard, H. Deleuze, Z. Saadi, R. Backov, Rational design of macrocellular silica scaffolds obtained by a tunable sol–gel foaming process, Adv. Mater. 16 (2) (2004) 140–144.
[2] P. Sepulveda, Gelcasting foams for porous ceramics, Am. Ceram. Soc. Bull. 76 (10) (1993) 61–65.
[3] M. Scheffler, P. Colombo, Cellular Ceramics: Structure, Manufacturing, Properties and Applications, Wiley-VCH, UK, 2005.
[4] D. Liu, Preparation and characterisation of porous hydroxyapatite bioceramic via a slip-casting route, Ceram. Int. 24 (6) (1998) 441–446.
[5] S. Kato, Y. Hirano, M. Iwata, T. Sano, K. Takeuchi, S. Matsuzawa, Photocatalytic degradation of gaseous sulfur compounds by silver-deposited titanium dioxide, Appl. Catal. B: Environ. 57 (2005) 109–115.
[6] H. Nagadomi, T. Takahasi, K. Sasaki, H.C. Yang, Simultaneous removal of chemical oxygen demand and nitrate in aerobic treatment of sewage wastewater using an immobilized photosynthetic bacterium of porous ceramic plates, World J. Microbiol. Biotechnol. 16 (2000) 57–62.
[7] A. Zampieri, P. Colombo, G.T.P. Mabande, T. Selvam, W. Schwieger, F. Scheffler, Zeolite coatings on microcellular ceramic foams: a novel route to microreactor and microseparator devices, Adv. Mater. 16 (9–10) (2004) 819–823.
[8] P. Sepulveda, J.G.P. Binner, Processing of cellular ceramics by foaming and in situ polymerization of organic monomers, J. Eur. Ceram. Soc. 19 (12) (1999) 2059–2066.
[9] P. Colombo, Ceramic foams: fabrication, properties and applications, Key Eng. Mater. 206–213 (2002) 1913–1918.

[10] H. Peng, A.Y. Tremblay, D.E. Veinot, The use of backflushed coalescing microfiltration as a pretreatment for the ultrafiltration of bilge water, Desalination 181 (1–3) (2005) 109–120.
[11] K.A. Hing, Bioceramic bone graft substitutes: influence of porosity and chemistry, Int. J. Ceram. Technol. 2 (3) (2005) 184–199.
[12] H. Maekawa, J. Esquena, S. Bishop, C. Solans, B.F. Chmelka, Meso/macroporous inorganic oxide monoliths from polymer foams, Adv. Mater. 15 (7–8) (2003) 591–596.
[13] D.A. Hirschfeld, T.K. Li, D.M. Liu, Processing of porous oxide ceramics, Key Eng. Mater. 115 (1996) 65–80.
[14] A.C. Pierre, Porous sol–gel ceramics, Ceram. Int. 23 (1997) 229–238.
[15] T. Higuchi, K. Kurumada, S. Nagamine, A.W. Lothongkum, M. Tanigaki, Effect of addition of polymeric species with ether moieties on porous structure of silica prepared by sol–gel method, J. Mater. Sci. 35 (2002) 3237–3243.
[16] W.L. Cui, Performance improvement of fused silica ceramics, Master Thesis, The Wuhan University of Science and Technology, 2002.
[17] D. Myers, Surfaces, Interfaces and Colliods: Principles and Applications, second ed., Wiley-VCH, UK, 1999.
[18] P. Sepulveda, F.S. Ortega, M.D.M. Innocentini, C. Pandolfelli, Properties of highly porous hydroxyapatite obtained by the gelcasting of foams, J. Am. Ceram. Soc. 83 (12) (2000) 3021–3024.
[19] P. Colombo, J.R. Hellmann, D.L. Shelleman, Mechanical properties of silicon oxycarbide ceramic foams, J. Am. Ceram. Soc. 84 (10) (2001) 2245–2251.
[20] F.A.C. Oliveira, S. Dias, M.F. Vaz, J.C. Fernandes, Behaviour of open-cell cordierite foams under compression, J. Eur. Ceram. Soc. 26 (1–2) (2006) 179–186.
[21] L.J. Gibson, M.F. Ashby, Cellular Solids: Structure and Properties, second ed., Cambridge University Press, UK, 1997.